

Simulations of flow-like landslides invading urban areas: a cellular automata approach with SCIDDICA

Valeria Lupiano^{1,2}  · Guillermo E. Machado³ · Lorena P. Molina^{3,4} · Gino M. Crisci¹ · Salvatore Di Gregorio⁵

Published online: 21 July 2017
© Springer Science+Business Media B.V. 2017

Abstract Different methodologies are used for modelling flow-like landslides. A common critical point concerns the flooding into town areas, which cannot be assimilated straight to a morphology, especially, when the urban tissue is very irregular with narrow streets and odd setting of buildings, so that discretization processes of approximating numerical methods have to be carefully examined in their limits. A semi-empirical approach by the computational paradigm of cellular automata is here considered with SCIDDICA, a competitive (related to PDE approach) cellular automata model for 3-dimensions simulation of flow-like landslides. This paper presents innovations to the transition function of SCIDDICA-SS2, which manage

opportune building data in the cells corresponding to the urban tissue. The novelties of the transition function need a theorem, here demonstrated which regards the Algorithm of Minimization of Differences in the new context of inhomogeneous cells. This progress permits to simulate the complete evolution of landslides, from the detachment area to its exhaustion almost on the same precision level. This is an advantage for hazard and risk analyses in threatened zones. Improved SCIDDICA-SS2 was applied successfully to all the well-known 2009 debris flows of Giampilieri Superiore (Sicily) also in comparison with simulation results of the previous versions.

Keywords Cellular automata · Modelling and simulation · Debris flow · Natural hazard · SCIDDICA · Giampilieri Superiore

✉ Valeria Lupiano
valeria.lupiano@unical.it; valeria.lupiano@irpi.cnr.it

Guillermo E. Machado
gmachado@unach.edu.ec

Lorena P. Molina
lmolina@unach.edu.ec; lmolina@epoch.edu.ec

Gino M. Crisci
crisci@unical.it

Salvatore Di Gregorio
salvatore.digregorio@unical.it

¹ Department of Biology, Ecology and Earth Sciences, University of Calabria, 87036 Rende, Italy

² National Research Council, Research Institute for Geo-Hydrological Protection, 87036 Rende, Italy

³ National University of Chimborazo, Faculty of Engineering, Riobamba, Ecuador

⁴ Polytechnic High School of Chimborazo, Faculty of Computer Science and Electronics, Riobamba, Ecuador

⁵ Department of Mathematics and Computer Science, University of Calabria, 87036 Rende, Italy

1 Introduction

Flow-like landslides of different types: debris flows, mudflows, lahars, rock avalanches are extremely dangerous surface flows, that can generate destructions with casualties in inhabited areas, especially in urban zones. Modelling and simulations of such natural disasters could be an important tool for hazard and risk mitigation and management in threatened regions.

Such complex fluid-dynamical phenomena are modelled through different standard approaches: empirical models, based on smart correlations of phenomenon observables, simple rheological and hydrological models, which assume acceptable simplifications, numerical methods approximating PDE (Hunggr 2009). These various approaches can produce discordant results (Canuti et al. 2002), because different objectives of the simulations could involve

different levels of precision for different types of data. Simulation results have to be accurately interpreted according to the model features. Simulations produce usually a large amount of data, whose usage in validation stage is devoted to a comparison with real event data, which are generally approximate in the evolution phase, but usually detailed for the final effects, that represent secure comparison terms.

Cellular automata (CA) represent an alternative numerical method for modelling dynamical complex systems, which evolve on the basis of local interactions of their constituent elements. A Cellular Automaton evolves in a discrete space–time. Space is partitioned in cells of uniform size, each cell embeds a finite states automaton (a computing unit), all the cells change simultaneously state according to a transition function of the states of the neighbour cells, where the neighbourhood conditions are determined by a pattern invariant in time and space (Di Gregorio and Serra 1999). An extension of classical CA, MCA, Multicomponent (alias Macroscopic) CA, was developed in order to model large scale (extended for kilometres) phenomena (Avolio et al. 2012; Di Gregorio and Serra 1999). MCA need a large amount of states, in order to describe “macroscopic” properties of the space portion corresponding to the cell; such states may be formally represented by means of sub-states (e.g., sub-state altitude, i.e., the average value of altitude in the cell), that specify the characteristics to be attributed to the state of the cell. This involves several advantages in the case of surface flows; quantities concerning the third dimension, i.e., the height, may be easily included among the MCA sub-states, e.g., the thickness of debris in the cell, permitting models in two dimensions, working effectively in three dimensions; limits of discreteness may be partially overcome, permitting valid refinements; e.g., debris in a cell can be expressed as a thickness, but a further specification could be introduced by specifying the sub-states “centre mass coordinates”.

Two MCA models were developed for flow-like landslide, SCIDDICA (several versions since 1987, (e.g., Avolio et al. 2008, 2013; Barca et al. 1987; Lupiano et al. 2014, 2015a; Mazzanti et al. 2010) for subaerial/subaqueous debris/mud/granular flows and LLUNPIY for primary and secondary lahars (Lupiano et al. 2014, 2015b, c; Machado et al. 2015a, b).

A critical point of these models concerns the flooding of town areas; previous solutions assimilated the urban tissue to a morphology and provided for a cell dimension small enough to permit that the cell corresponds nearly entirely to a piece of the road-bed (altitude of the road-bed) or to a piece of building (altitude of the building).

When part of the urban tissue consists of narrow streets and very irregular setting of buildings, due to historical

contingencies, such a solution could involve an extremely large amount of cells, if the complete evolution of landslides from the detachment area to its exhaustion has to be simulated. That could implicate unsustainable computing time with the number of cells multiplied at least some hundreds times, if we consider that the model validation and following hazard analyses can imply thousands of simulations (D’Ambrosio et al. 2013b).

Preliminarily in order to overcome these problems, a generalization of AMD (the algorithm of minimization of differences (Avolio et al. 2012), first step for determining cell outflows) to inhomogeneous (in size) cells was specified and the corresponding theorem was demonstrated.

AMD is the basis for many CA models of surface flows: lava flows (Crisci et al. 2008, 2010; D’Ambrosio et al. 2013a), pyroclastic flows (Crisci et al. 2005), soil erosion by rainfall (D’Ambrosio et al. 2001; Valette et al. 2006), hot mudflows (Arai and Basuki 2010); long-term soil redistribution by tillage (Vanwalleghem et al. 2010); sandy shore erosion (Calidonna et al. 2016); snow avalanche (Barpi et al. 2007; Avolio et al. 2017); density currents (Salles et al. 2007) and, at last, debris/mud/granular flows and lahars with models SCIDDICA and LLUNPIY (Lupiano et al. 2014, 2015b, c; Machado et al. 2015a, b).

SCIDDICA-SS2 (Avolio et al. 2008; Mazzanti et al. 2010), SCIDDICA-SS3 (Avolio et al. 2013; Lupiano et al. 2014, 2015a) and LLUNPIY (Lupiano et al. 2014, 2015b, c; Machado et al. 2015a, b) are our front-rank models for simulations of flow-like landslides.

An extension of SCIDDICA-SS2 (Avolio et al. 2008; Mazzanti et al. 2010) was developed by introducing the generalized AMD; a new sub-state, which encodes building data, is introduced and the new version of the AMD was applied in order to account for different heights (part of the road-bed, parts of buildings) inside the same cell and for two cases, that concern the building positions related to the division of the space in cells; we consider two adjacent cells A, B and possible flows from A to B:

- part of the common edge to two adjacent cells is at the level that is the minimum height level for the cell B (the road-bed), so that flows can invade higher parts of B after the lower parts;
- all the common edge is at a level, that is not the minimum height level for the cell B (one or more buildings occupy the edge); it involves that flows can arrive to the lower parts of B only after invading the higher part; it implies the introduction of a threshold value that accounts for that in computation.

Such an extension was applied for simulating the well-known catastrophic landslide that overran Giampileri Superiore in 2009. This version of SCIDDICA was able to

simulate with excellent results the complex event (many detachment areas, many streams flow together and branch in the town) just from beginning.

The extended version of AMD together with the demonstration of the theorem and application for urban cells is specified in the next section.

A short presentation of SCIDDICA-SS2 is specified in the third section, the fourth section reports and compares different simulations of Giampileri Superiore debris flows, conclusions and comments appear at the end.

2 AMD adaptation to inhomogeneous cells

The AMD (Di Gregorio and Serra 1999; Avolio et al. 2012) is here adapted to inhomogeneous situations, which may be intuitively made explicit in the following way: n cells in the neighbourhood, to which are attributed different areas and quantities in terms of height, m ($m < n$) cells are “central” cells, i.e., cells with moreover quantities (always in terms of height), which are distributable to the neighbourhood. The quantity to be minimized by this expanded version of AMD is the “differences of height”.

2.1 AMD theorem for inhomogeneous cells

AMD adaptation to inhomogeneous cells is formally specified according to Tables 1 and 2.

Theorem *The algorithm of minimization of the differences (AMD or shortly minimization algorithm) computes values of f'_i $1 \leq i \leq n$, such that (1) is minimized.*

Proof It will be demonstrated that each distribution f''_i , $1 \leq i \leq n$, $\sum_{1 \leq i \leq n} f''_i = \sum_{1 \leq j \leq m} d_j a_j$, different from the minimization algorithm one, with $h''_i = h_i + f''_i$ $1 \leq i \leq n$ involves that

$$\sum_{\{(v,w)|1 \leq v < w \leq n\}} |h''_v - h''_w| > \sum_{\{(v,w)|1 \leq v < w \leq n\}} |h'_v - h'_w| \tag{2}$$

Differences $\Delta_i = h''_i - h'_i$ $1 \leq i \leq n$ imply $\sum_{1 \leq i \leq n} \Delta_i a_i = 0$. A different distribution f''_i $1 \leq i \leq n$ involve some (at least one) $\Delta_x > 0$ to be counterbalanced by some (at least one) $\Delta_y < 0$.

A different distribution involves that $\Delta_i \geq 0$ for $i \notin A$ because $f'_i = 0$ and $f''_i \geq 0$; $\Delta_i > 0$ for $i \in A$ implies $h''_i > h_i$; value $\Delta_i < 0$ can be assumed only for cells $i \in A$ because $f'_i > 0$ and $f''_i \geq 0$ permits cases with $f'_i > f''_i$.

Let $C = \{r | (\Delta_r = 0) \wedge (1 \leq r \leq n)\}$, $C' = \{s | (\Delta_s > 0) \wedge (1 \leq s \leq n)\}$, $C'' = \{t | (\Delta_t < 0) \wedge (1 \leq t \leq n)\}$ and $D = \sum_{s \in C'} \Delta_s a_s$; $\sum_{s \in C'} \Delta_s a_s + \sum_{t \in C''} \Delta_t a_t = 0$, $\sum_{s \in C'} \Delta_s a_s = -\sum_{t \in C''} \Delta_t a_t$, $D = -\sum_{t \in C''} \Delta_t a_t$. Note that $C'' \subseteq A$.

It is possible to pass step by step from the minimisation algorithm distribution to another distribution by consecutive q shifts $\zeta_{j,i} = -\Delta_j a_j \Delta_i a_i / D$ from each cell j of C' to each cell i of C'' , so that each shift is proportional both to Δ_i and Δ_j .

$$\sum_{i \in C''} \zeta_{j,i} = -\sum_{i \in C''} \Delta_j a_j \Delta_i a_i / D = -\Delta_j a_j \text{ and } \sum_{j \in C'} \zeta_{j,i} = -\sum_{j \in C'} \Delta_j a_j \Delta_i a_i / D = \Delta_i a_i.$$

Let $\zeta_{u,v}$ be a shift with $u \in C'$, $v \in C''$, ${}^b h_i$, ${}^a h_i$ quantities in the cell i $1 \leq i \leq n$ respectively before ^(b) and after ^(a) the shift $\zeta_{u,v}$.

Note that ${}^b h_i \geq h_i$, $i \in C'$ then ${}^b h_v \geq h_v$; ${}^b h_j \leq h_j$, $j \in C''$ then ${}^b h_u \leq h_u$; ${}^b h_k \geq h_k$ $k \in C$.

For v and u : $|{}^a h_v - {}^a h_u| = |({}^b h_v + \zeta_{u,v} / a_v) - ({}^b h_u - \zeta_{u,v} / a_u)| = |{}^b h_v - {}^b h_u + \zeta_{u,v} / a_v + \zeta_{u,v} / a_u| > |{}^b h_v - {}^b h_u|$ because ${}^b h_v \geq {}^b h_u$; $\{t | t \in C'\}$: $|{}^a h_v - {}^a h_t| = |{}^b h_v + \zeta_{u,v} / a_v - {}^b h_t| = ({}^b h_v - {}^b h_t) + \zeta_{u,v} / a_v$ because ${}^b h_v \geq {}^b h_t$; $|{}^a h_u - {}^a h_t| = |{}^b h_u - \zeta_{u,v} / a_u - {}^b h_t| \geq ({}^b h_u - {}^b h_t) - \zeta_{u,v} / a_u$; minimum value of $|{}^a h_u - {}^a h_t|$ when ${}^b h_u = \zeta_{u,v} / a_u + {}^b h_t$ therefore $({}^a h_v - {}^a h_t) + ({}^a h_u - {}^a h_t) \geq ({}^b h_v - {}^b h_t) + ({}^b h_u - {}^b h_t)$ $\{t | t \in C' \vee t \in C\}$: $|{}^a h_u - {}^a h_t| = |{}^b h_u - \zeta_{u,v} / a_u - {}^b h_t| = ({}^b h_u -$

Table 1 AMD specification for inhomogeneous cells

Definitions	n cells of the neighborhood; m “central” cells (the first m indexes are reserved to these cells) h_i = height of the not distributable quantity in the cell i $1 \leq i \leq n$ a_i = area of the cell i $1 \leq i \leq n$ d_j = height of the distributable quantity in the cell j $1 \leq j \leq m$. f'_i = total flow (volume) from the central cells towards the cell i $1 \leq i < n$ and/or the part of d_j remaining in the central cell j $1 \leq j \leq m$. $h'_i = h_i + f'_i / a_i$ $1 \leq i < n$ new height of the cell after the flows contribution
Bound	$\sum_{1 \leq i \leq n} f'_i = \sum_{1 \leq j \leq m} d_j a_j$
Problem	f'_i $1 \leq i \leq n$ must be determined in order to minimize the sum of the height differences between all the pairs of cells in the neighborhood: $\sum_{\{(v,w) 1 \leq v < w \leq n\}} h'_v - h'_w \tag{1}$

Table 2 Algorithm of Minimization of the Difference for inhomogeneous cells

Initialization	a) All the neighboring cells are considered “admissible” to receive flows from the central cells, A is the set of admissible cells
Cycle	b) The “average height” (\bar{h}) is found for the set A of admissible cells: $\bar{h} = (\sum_{1 \leq j \leq m} d_j a_j + \sum_{k \in A} h_k a_k) / \sum_{k \in A} a_k$ c) Each cell x with $h_x \geq \bar{h}$ is eliminated from the set A
End of cycle	d) Go to step-b) until no cell is eliminated
Result:	e) $f'_k = a_k (\bar{h} - h_k)$ for $k \in A$ ($h_k < \bar{h}$); $f'_k = 0$ for $k \notin A$ ($h'_k \geq \bar{h}$)
Bound conservation	$\sum_{k \in A} f'_k = \sum_{k \in A} a_k (\bar{h} - h_k) = \bar{h} \sum_{k \in A} a_k - \sum_{k \in A} (a_k h_k) = (\sum_{1 \leq j \leq m} d_j a_j + \sum_{k \in A} h_k a_k) / \sum_{k \in A} a_k (\sum_{k \in A} a_k) - \sum_{k \in A} h_k = \sum_{1 \leq j \leq m} d_j a_j$
Properties	P1: $h'_k = f'_k / a_k + h_k = \bar{h} - h_k + h_k = \bar{h}$ for $k \in A$ P2: $h'_k = h_k$ because $f'_k = 0$ for $k \notin A$

${}^b h_t + \zeta_{u,v}/a_u$ because ${}^b h_t \geq {}^b h_u$; $|{}^a h_v - {}^a h_t| = |{}^b h_v + \zeta_{u,v}/a_v - {}^b h_t| \geq (|{}^b h_v - {}^b h_t| - \zeta_{u,v}/a_v)$; minimum value of $|{}^a h_u - {}^a h_t|$ when ${}^b h_t = \zeta_{u,v}/a_v + {}^b h_v$ therefore $(|{}^a h_v - {}^a h_t| + |{}^a h_u - {}^a h_t|) \geq (|{}^b h_v - {}^b h_t| + |{}^b h_u - {}^b h_t|)$

$$\{(u, t) | u \neq v, t \neq u\} : (|{}^a h_u - {}^a h_t|) = (|{}^b h_u - {}^b h_t|)$$

therefore $\sum_{\{(i,j) | 0 \leq i < j \leq n\}} (|{}^a h_i - {}^a h_j|) > \sum_{\{(i,j) | 0 \leq i < j \leq n\}} (|{}^b h_i - {}^b h_j|)$

We obtain h_i'' $1 \leq i \leq n$ by consecutive applications of all the shifts $\zeta_{j,i}$ $j \in C''$, $i \in C'$ starting from h_i' $1 \leq i \leq n$; then (2) is proved.

2.2 Specification of the extended AMD for urban areas

The altitude sub-state in AMD (Avolio et al. 2012; Di Gregorio and Serra 1999) application to surface flows is specified as the average altitude of the area corresponding to the cell. This approximation is evidently valid for simulation in the cases, where don't exist decidedly differentiate levels as ground level and building level. But if such an approximation is applied to an urban tissue for cells with relevant parts at more than one level, a town could be distorted into a hill where surface flows cannot invade streets. The problem of differentiate levels may be overcome by reducing the cell dimensions to much less than the width of streets. In such a case the average altitude approach could work. In the same conditions, if only a level is considered representative of the cell altitude (the other levels take a minor part of the cell), such an approximation permits to simulate flows penetrating the town through the streets. These solutions with reduced size cell could be revealed rough or often impracticable especially when the urban tissue is very irregular with narrow streets and odd setting of buildings, which reflect historical contingencies. Furthermore an extremely large amount of cells could be necessary, if the complete evolution of flow like landslides has to be simulated from the detachment area to its exhaustion according to the adopted simulation criteria.

That could involve unsustainable computing time with number of cells multiplied at least some hundreds times, if we consider that the model validation and following hazard analyses can imply thousands of simulations.

AMD was expanded in order to account for different altitudes (part of the road-bed, parts of buildings) inside the same cell.

In the case of different altitude levels inside the same cell, it may be decomposed in as many cells as the altitude levels with different areas, whose value is related to the part of the cell at that altitude level.

Such AMD version is complete in comparison with the previous one (Lupiano et al. 2016), where only two levels road-bed and building were considered.

The application of AMD to a neighborhood, where the cells are at the same altitude, but have different areas, is not straightforward, because it is possible a situation where a cell may be invaded by an outflow from the central cell only after another neighbor cell at higher altitude is invaded.

This is the case of a cell that “borders” only on cells at higher altitude; e.g., a cell corresponding to the road-bed part, that doesn't “border” on the central cell, but only with cells, corresponding to the building parts at higher altitude. So an outflow from central cell can reach the “road-bed” cell after flooding the lowest “building” cell. There is a threshold to overcome for such cases: the altitude of such lowest cell; then it is necessary to associate a threshold value for each neighbor cell in order to account for that.

If a threshold is added to each neighborhood cell (the more frequent case is a null threshold), extended AMD may be used as many times as the number of different thresholds in order to manage such complex cases.

The following intuitive reasoning accounts for the computation procedure, then formal specifications for AMD application are given in Table 3 and the general pseudocode (C-like) for outflows determination is shown in Table 4.

Let us consider thresholds in increasing order and get started from the lowest threshold (the first reference threshold Thr , which is always null); all the cells with

Table 3 Definitions for application of AMD extension to urban areas

n	Number of cells in the neighborhood
d	Distributable quantity in the neighborhood
h_i	Height of the neighbor cell i , $0 \leq i \leq n$
a_i	Area of the neighbor cell i , $0 \leq i \leq n$
t_i	Threshold related to the neighbor cell i , $0 \leq i \leq n$
A_i	The neighbor cell i , $0 \leq i \leq n$ is admissible to receive flows from the central cells (<i>true</i> or <i>false</i>)
H_i	Alias for height of the neighbor cell i , $0 \leq i \leq n$
D	Alias for distributable quantity in the neighborhood
f_i	Flow toward the neighbor cell i , $0 \leq i \leq n$
h	Average height
h'_i	$h'_i = h_i + f_i/a_i$, $0 \leq i \leq n$

larger threshold are not considered admissible and AMD is applied in such a situation.

If the average height do not overcome the next threshold, outflows cannot reach cells at lower level with such threshold value and minimizing flows are definitively determined (exit conditions); differently outflows reach the cells with next threshold value after filling the remaining admissible cells.

This last situation involves a new computation: outflows are assigned to the remaining admissible cells until their height reaches the next threshold value, which becomes the new reference threshold value; so their new height is the next threshold value, the distributable quantity is reduced by accounting for the assigned outflows.

Now AMD could be applied again with the new *Thr* and the new heights. Of course AMD applications are iterated in such a way until minimizing flows don't overcome the value of a reference threshold or the maximum threshold is considered.

AMD is extended in order to manage the lack of homogeneity regarding the different altitudes for parts of the same cell. It involves a distinction of different rates of the cell area (normalized to unit), to which different altitudes correspond.

The specification of AMD in Table 4 may be applied in the following to two-dimensions CA with hexagonal tessellation (e.g., SCIDDICA-SS2, SCIDDICA-SS3, LLUNPIY) with cells divided in more parts with areas of different altitude. Preliminary definitions are given in Table 3. Alias are used in order to save initial values, which could change during the execution of the algorithm.

3 SCIDDICA-SS2 extension to urban areas

SCIDDICA-SS2 (Avolio et al. 2008; Iovine et al. 2007; Mazzanti et al. 2010), SCIDDICA-SS3 (Avolio et al. 2013; Lupiano et al. 2014, 2015a) and LLUNPIY (Lupiano et al. 2014, 2015b, c; Machado et al. 2015a, b) are our front-rank

models for simulations of flow-like landslides. They are two-dimensions hexagonal CA (Fig. 1), but they work really in three dimensions: the grid is a projection onto a horizontal plane, where the third dimension is specified by sub-states (Table 3), hexagonal cells guarantee the maximum reduction of problems of spurious symmetries. The results of updating cells are the same of an updating for a parallel synchronous computation, using double matrices for sequential computers.

The extension of SCIDDICA-SS2 to urban areas and applied to Giampilieri Superiore events, could be introduced easily in SCIDDICA-SS3, that represents a more precise version, but involving long running times, or in LLUNPIY, an adaptation of SCIDDICA-SS3 to lahar features. The following description of SCIDDICA-SS2 considers only the part of subaerial flows, without lacking of generality; a successive section presents the extended AMD.

3.1 Main specifications of SCIDDICA-SS2

The hexagonal CA model SCIDDICA-SS2 is the quintuple: $\langle R, X, S, P, \tau \rangle$ where:

- $R = \{(x, y) | x, y \in \mathbb{N}, 0 \leq x \leq l_x, 0 \leq y \leq l_y\}$ is the set of points with integer coordinates, that individuate the regular hexagonal cells, covering the finite region, where the phenomenon evolves. \mathbb{N} is the set of natural numbers.
- $X = \{(0, 0), (1, 0), (0, 1), (-1, 1), (-1, 0), (0, -1), (-1, -1)\}$, the neighborhood index, identifies the geometrical pattern of cells, which influence state change of the central cell: the central cell (index 0) itself and the six adjacent cells (indexes 1,,6).
- S is the finite set of states of the finite automaton, embedded in the cell; it is equal to the Cartesian product of the sets of the considered sub-states (Table 5). The new sub-state C specifies the type of cell: normal cell; detachment cell, where the landslide originates (the detachment depth is encoded in the

Table 4 The general pseudocode (C-like) for outflows determination

```

{ D=d; //alias for the distributable quantity
  for (i=1; i≤n; i++)
  { Hi=hi ; //alias for the heights of cell i
    fi=0; //initialization for outflow toward cell i
  }
  Thr=0; //initial reference threshold
  do //general cycle beginning
  { for (i=1;i≤n; i++)
    Ai=ti≤Thr //admissibility determination
  } do //AMD cycle beginning
  { sum=D; //initialization of sum for h determination
    totArea=0; //total Area of admissible cells initialization
    exclusion=false; //no exclusion initially
    for (i=1;i≤n; i++)
      if (Ai) //if cell i is admissible
      { sum=sum+Hi*ai; //sum of weighted heights updating
        totArea=totArea+ai; //totArea updating
      }
    h=sum/totArea; //average height determination
    for (i=1;i≤n; i++)
      if (Ai∧(Hi>h)) //if height of cell i overcomes h
      { Ai=false; //cell i is no more admissible
        exclusion=true; //exclusion occurs
      }
    } while(exclusion); //repeat until exclusion occurs
    newThr=h; //upper limit of the new reference threshold
    new_cycle=false; //initialization of new_cycle
    for (i=1;i≤n; i++)
      if ((ti<h)∧(ti>Thr)) //possible reference threshold check
      { new_cycle=true; //a new cycle is necessary
        if (ti<newThr) newThr=ti; //new lower value for newThr
      }
    if (new_cycle)
    { Thr=newThr; //reference threshold updating
      for (i=1;i≤n; i++)
        if (Ai) //if cell i is admissible
        { fi=fi+(Thr-Hi)*ai; //outflow toward cell i updating
          D=D-(Thr-Hi)*ai; //distributable quantity reduction
          Hi=Thr; //height of cell i updating
        }
      }
    else
      for (i=1;i≤n; i++)
        if (Ai) fi=fi+(h-Hi)*ai; //final outflow toward cell i
    } while (new_cycle);
  }
}

```


Fig. 1 **a** Hexagonal neighbourhood with coordinates; **b** indexes of cells of the neighbourhood

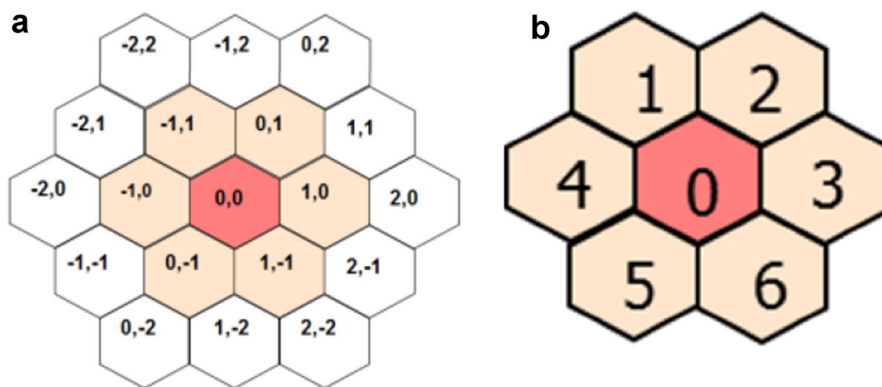


Table 5 Sub-states

Sub-states	Description
C, A, D	Type of cell, cell altitude, erodible soil depth,
T, X, Y, K	Debris thickness, co-ordinates X and Y of the debris barycenter inside the cell, kinetic head,
E_T, E_X, E_Y, E_K (6 components)	External debris flow normalized to a thickness, external flow co-ordinates X and Y , kinetic head of external flow
I_T, I_X, I_Y, I_K (6 components)	Internal debris flow normalized to a Thickness, Internal flow co-ordinates X and Y , kinetic head of internal flow

C value); “urban” cell, whose C value encodes the road-bed and building altitudes together with the percentages of the parts of cell at different altitudes.

- P is the set of the global physical and empirical parameters (Table 6), which account for the general frame of the model and the physical characteristics of the phenomenon, the choice of some parameters is imposed by the desired precision of simulation where possible, e.g., cell dimension; the value of some parameters is deduced by physical features of the phenomenon, e.g., turbulence dissipation, even if an acceptable value is fixed by the simulation quality by attempts, triggered by comparison of discrepancies between real event knowledge and simulation results.
- $\tau: S^7 \rightarrow S$ is the cell deterministic state transition, it accounts for the components of the phenomenon, the “elementary processes” that are sketched in the next section.

Table 6 Physical and empirical parameters (with their physical dimensions)

Parameters	Description
a, t	Cell apothem (m), temporal correspondence to a CA step (s)
p_f	Friction coefficient parameter (°)
d, d_e, p_e, t_m	Energy dissipation by turbulence (–) and erosion (–); parameter of progressive erosion (–); mobilization threshold (m)

3.2 Outline of SCIDDICA-SS2 transition function

A MCA step involves the ordered application of the following elementary processes, which constitute the transition function; every elementary process implies the state updating. In the formulae, neighborhood index for sub-states and related variables is specified by subscript, if it is not referred to central cell; ΔQ means Q value variation, multiplication is explicitly “.”.

Debris outflows Outflows computation is performed in two steps: determination of the outflows f_i towards the cell $i, 1 \leq i \leq n$ (related to the different height levels of the cells in the hexagonal neighborhood) by the new AMD (described in Sect. 2) according to the different elevations of the neighborhood cell and determination of the shift of the outflows (Avolio et al. 2008, 2012; Mazzanti et al. 2010).

Initial data for computing minimizing flows by AMD are the following:

- a_i area rate related to the cell $i, 1 \leq i \leq n$
- e_i elevation (altitude) related to the cell $i, 1 \leq i \leq n$
- $h_i = e_i + K_0$ if cell i is a sub-cell of the central cell
- $h_i = e_i + T_j$ if cell i is a sub-cell of the adjacent cell $j, 1 \leq j \leq n$
- t_i threshold related to the cell $i, 0 \leq i \leq n$
- $d = T_0$ distributable quantity in the central cell,

The outflow could be represented as an ideal cylinder, tangent the next edge of the central hexagonal cell, whose barycenter corresponds to the debris barycenter inside the

central cell, in direction to the center of the neighbor cell. The part of the outflow, that overcomes the central cell, constitutes the external flow, specified by external flow sub-states, while the remaining part, the internal flow, is specified by internal flow sub-states. Shift “ Δs ” is computed according to the following simple formula, that averages the movement of all the mass as the barycenter movement of a body on a constant slope θ with a constant friction coefficient: $\Delta s = v \cdot t + g \cdot (\sin\theta - p_f \cdot \cos\theta) \cdot t^2/2$ with “ g ” gravity acceleration and initial velocity $v = \sqrt{2 \cdot g \cdot K}$ (Avolio et al. 2008, 2013).

Turbulence effect A turbulence effect is modelled by a proportional kinetic head loss at each SCIDDICA step: $-\Delta K = d_t \cdot K$. This formula involves that a velocity limit is asymptotically imposed de facto, for a maximum slope value.

Soil erosion When the kinetic head value overcomes an opportune threshold ($K > t_m$), depending on the soil features, then a mobilization of the detrital cover occurs proportionally to the quantity overcoming the threshold: $p_e \cdot (K - t_m) = \Delta T = -\Delta D$ (the erodible soil depth diminishes as the debris thickness increases), the kinetic head loss is: $-\Delta K = d_e \cdot (K - t_m)$.

Flows composition When outflows and their shifts are computed, the new situation involves that external flows leave the cell, internal flows remain in the cell with different co-ordinates and inflows (trivially derived by the values of external flows of the neighbor cells) have to be added. The new value of T is given, considering the balance of inflows and outflows with the remaining debris mass in the cell. A kinetic energy reduction is considered by loss of flows, while an increase is given by inflows: the new value of the kinetic

Fig. 2 October 2009 debris flows occurred in Giampilieri Superiore



head is deduced from the computed kinetic energy. X and Y are calculated as the average weight of the co-ordinates considering the remaining thickness in the central cell, the thickness of internal flows and the inflows.

Such an extension was applied for simulating the well-known catastrophic landslide that overran Giampilieri Superiore in 2009. This version of SCIDDICA was able to simulate with excellent results the complex event (many detachment areas, many streams flow together and branch in the town) just from beginning.

4 Giampilieri superiore debris flow simulations

4.1 1st October 2009 landslides event

On the October 1st 2009 a severe meteorological event affected the Peloritani Mountains (NE Sicily). The intense rainfall caused floods and triggered many debris and mud flows that brought 37 fatalities, numerous injured, several damages to public and private buildings, railways, roads, infrastructures, electric and telephonic networks, thousands of evacuated persons. The Department of Civil Protection

of Sicilian Region mapped more than 600 landslides, in an area, that stretched approximately for 50 km². Analysis of the rainfall event indicates a cumulative rainfall depth of 225 mm obtained in 9 h from the data recorded at the S. Stefano di Briga rain-gauge, with a peak of rainfall intensity of about 22 mm/min. The area is susceptible to debris flows because of lithological characteristics, complex tectonic history, high gradient of slopes (30°–60°) and landscapes characterized by narrow gullies with torrential hydraulic regime (Ardizzone et al. 2012). In fact, the disaster occurred in an area with high hydrogeological risk, which was already hit previously by landslides and foods. Two years before, on October 2007, after a violent storm, a mud flow had invaded Giampilieri Superiore, causing elevated material damages, but without victims.

Giampilieri Superiore was one of the most wounded villages by October 1st 2009 catastrophic events. Much debris flow (Fig. 2) crossed the country causing destructions and casualties. The village is located on the eastern slopes of the Peloritani Mountains on left side of Giampilieri River. In particular, it rises on an alluvial fan and is crossed by various creeks, tributaries of the Giampilieri River. All of them are characterized by small catchments



Fig. 3 **a** View of Giampilieri Superiore village; **b** Vallone Street the day after the event; **c** example of Chiesa Street during a normal rainfall event

with extension ranging from 0.03 to 0.1 km² (Stancanelli et al. 2013; Stancanelli and Foti 2015).

Inside the urbanized area, the streams paths merges with street paths, so Loco Creek becomes Saccà Street, Sopra Urno Creek becomes Chiesa Street and Puntale Creek becomes Vallone Street (Fig. 3a–c).

During the paroxysmal pluvial event, debris flows (Fig. 2) were mobilized from the slope behind the village; many of these were channelled before to the drainage network and after to the riverbeds-street, when they reached Giampilieri Superiore and produced dramatic effects in terms of loss of human lives and damages of buildings. The severity of the rainfall event was not the only cause of the disaster. In fact, other factors contributed to slope failures in the Giampilieri Superiore case, as Ardizzone et al. (2012) stressed: abandoned terraced slopes lacking proper drainage and unmaintained dry walls.

4.2 Application of SCIDDICA SS2 to Giampilieri superiore debris flows

For testing the innovation introduced in SCIDDICA-SS2, we considered, initially, the Sopra Urno debris flows (marked with n.2 in Fig. 2), and subsequently the other three debris flows that crossed the urban area (marked with n.1, 3, and 4, in Fig. 2). SCIDDICA-SS2 and -SS3 were calibrated and validated (Lupiano et al. 2014, 2015b, c) on all debris flows occurred in Giampilieri Superiore area. The same parameters were used for simulations of this extended model. Genetic Algorithms (GA) were used for some key parameters related to energy dissipation in the previous versions of SCIDDICA; analogous applications of GA could improve simulation; more precisely, GA were used for SCIDDICA-SS2 just only for setting the two very sensitive parameters energy dissipation by turbulence (d_t)

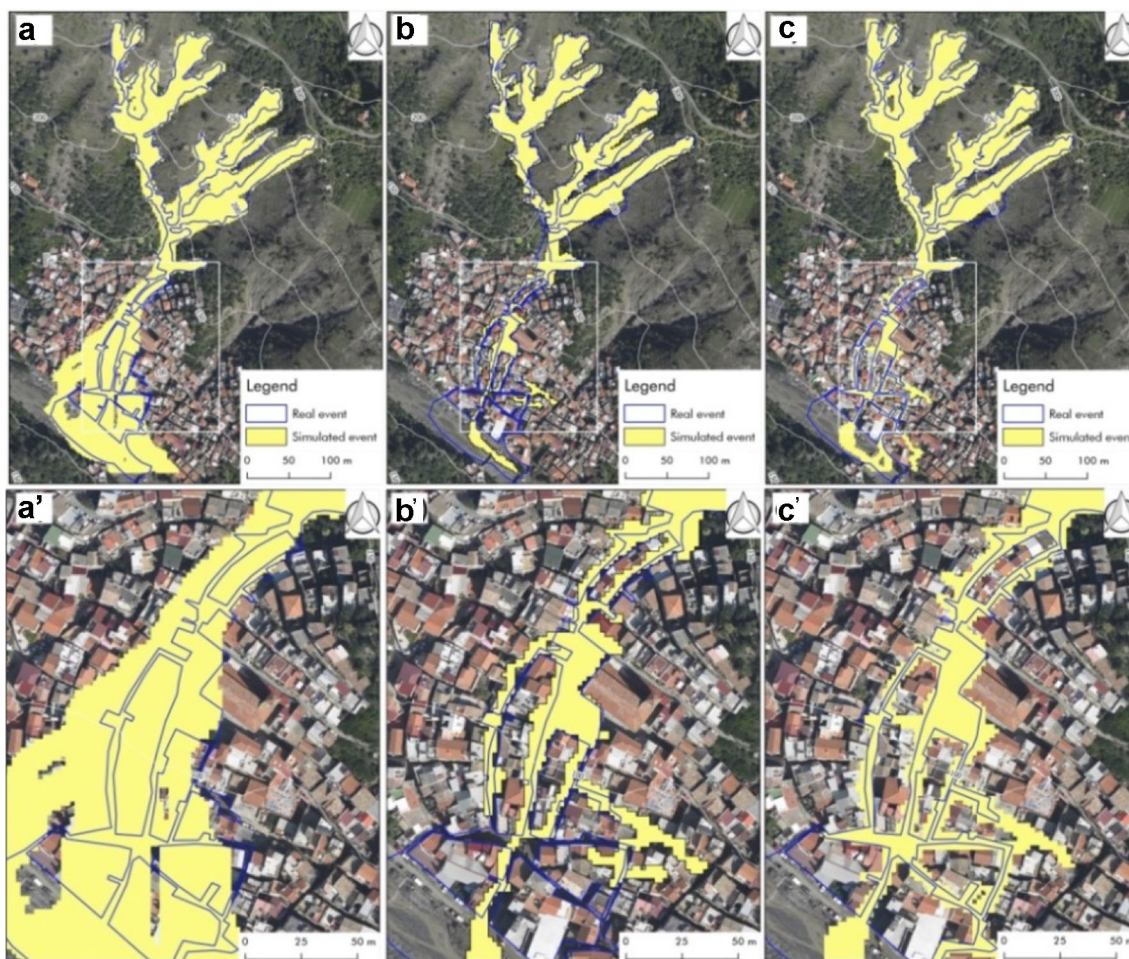


Fig. 4 Comparison among real event and simulated event: **a** on DTM; **b** on DEM; **c** simulated event considering the improvement introducing in SCIDDICA; **a'**, **b'** and **c'** enlargement of case **a**, **b** and **c** in urban area

and by erosion (d_c), because computation time cost for all the parameters would be prohibitive for our computation resources.

Three simulation experiments have been performed: the first one on a DTM (Digital Terrain Model), the second and third one on a DEM (Digital Elevation Model). Cell size is 2 m in both cases which corresponds an apothem of 1 m in hexagonal tessellation.

The terms DTM and DEM are often confused. The principal difference between the two digital models lies in the fact that the DEM takes into account all objects on the ground (vegetation, buildings and other artefacts), while the DTM shows the geodetic surface. The difference between the two models is more evident in urban areas where buildings prevail.

First experiment, shown in Fig. 4a, a': simulates the event, by considering the elevation at ground level in the urbanized area. The flows at the change of slope, reduce the speed, and give rise to the typical fan shape of debris.

A second test (Fig. 4b, b') was performed using a DEM, that was obtained from DTM manipulation by inserting urban data related to buildings and roads and by approximating altitude to road-bed, so that wider roads are considered in some cells. The flows, when reach the urbanized area, insinuate among the buildings. This approximation could involve in comparison with the real event that a larger rate of debris can flow along the steeply sloping "widened" roads and consequently a more limited expansion toward lateral roads with less slope.

The results show a good capability of the model to simulate the debris run-out, particularly, in the upper parts of the basins, while in the urbanized area, the reproduction of the real events is less accurate. In fact, significant differences do exist in the lateral spreading characteristics of the run-out, as the debris penetration inside lateral streets in the real event is larger than in simulation results. This is related to both the inevitable approximation errors in the process of data elaboration from square cells to hexagonal cells, and to DEM accuracy. The presence of buildings in urban areas involves a greater difference of elevation between the ground and the same buildings, for the same corresponding cell. This induces an approximation in the assessment of the average elevation of cells that are partially covered by a building and by a terrain or a street. Results show that the program could be refined in the

reproducing debris flow propagation into highly urbanized areas, where streets are narrow.

The third experiment is performed by simulations with SCIDDICA-SS2 extension for urban areas, where AMD adaptation to inhomogeneous cells is applied. A significant improvement had been obtained by the possibility of exploiting a better cell specification with two levels, the road-bed level and the building level together with the respective ratios.

It is possible to note (Fig. 4b', c') as the path of flows is better simulated in the urbanized areas, compared to the real event and to the simulations with the previous model versions, where some badly-hit lateral alleys turned out to be not inundated by detrital flows, just the opposite of the real event and simulations of the extended SCIDDICA-SS2. The duration times improve too; the real event lasted 5–6 min, the duration of simulations without AMD improvement is 10 min, while duration is 7 min with AMD improvement.

In Table 7 are reported the values of the evaluation (or fitness) function f , where R is the set of cells involved in the real event and S the corresponding one for simulated event. This function returns values from 0 (completely wrong simulation) to 1 (perfect match); values greater than 0.7 (precision lack in input data) are considered good results. The evaluation formula accounts for the necessity to compare results of different dimensions, so square (cubic) root normalizes surface (volume) measures.

In order to validate the innovations introduced, the simulations of the other three events that have passed through the village were performed. The application of the model returned the results shown in Figs. 5, 6, and 7. In the simulations based on a DTM (Fig. 5a–c) is possible to note how the flows are not influenced by presence of buildings in inhabited area. The situation improves with simulations performed on DEM (Fig. 6a–c) but best results are obtained with the improved model (Fig. 7a–c). The improvements are especially visible in the case of Puntale debris flow (Figs. 5b, 6b, 7b), rather than in the cases at the periphery of the village with few buildings.

The debris flow reported in Fig. 8 (marked as 5 in Fig. 2), named primary school debris flow, was deflected by the presence of the perimeter wall of the primary school. This wall has partially protected the building. In order to simulate this event, a wall was inserted on the DTM (4 m high and 2 m thick) as topographic alteration.

The simulation was performed in such a modified morphology and was compared with simulations without alterations. Figure 8a, b report the results of simulations without and with the presence of the wall. This application of SCIDDICA is very important, in fact the model may be used in order to verify the validity of protective barriers or trenches together with analysing the effects of diverted flows into other areas.

Table 7 Evaluation function f in Sopra Urno debris flow

	$f = \sqrt{\frac{R \cap S}{R \cup S}}$
On DTM	0.73
On DEM without improvement	0.77
On DEM with improvement	0.82

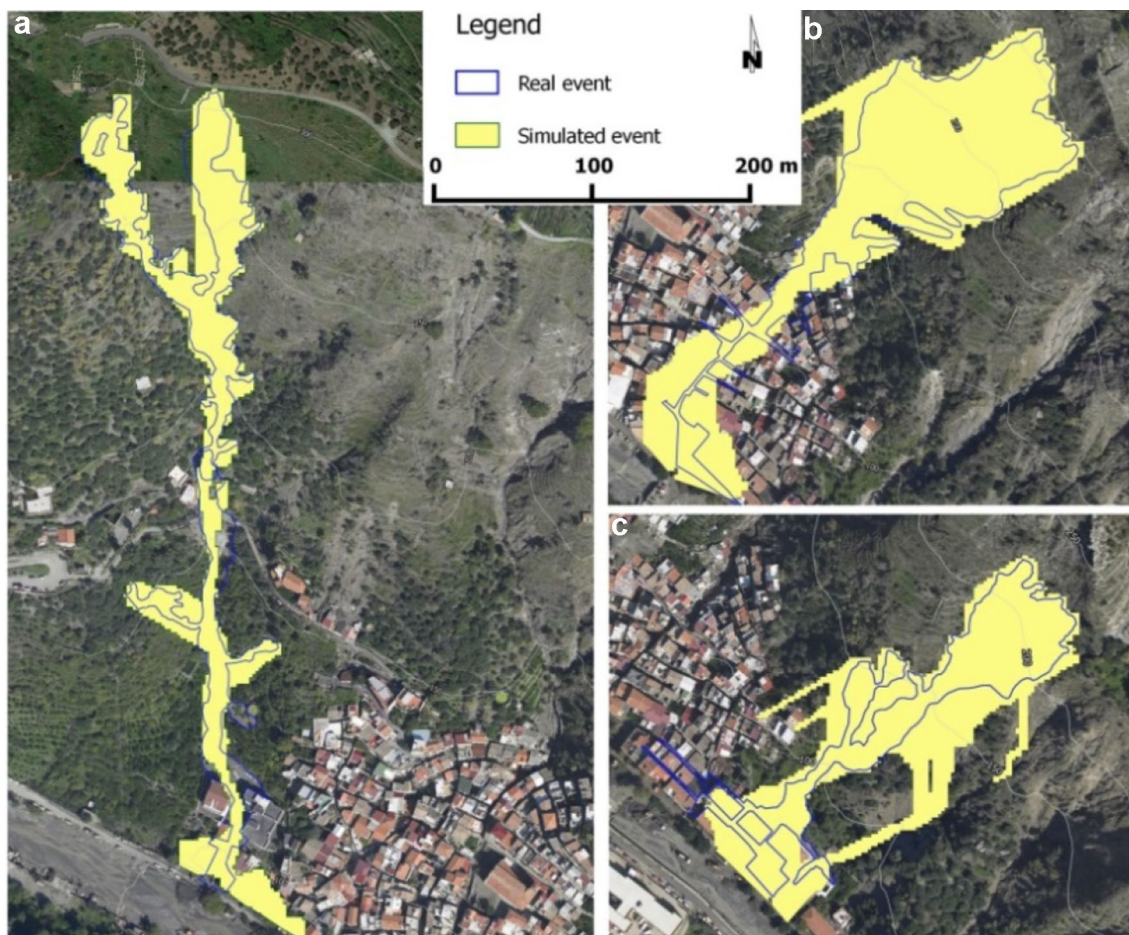


Fig. 5 Simulated events on DTM; **a** Loco creek debris flow; **b** Puntale Creek debris flow; **c** Lena Street debris flow

Table 8 reports the value of fitness function in such cases. Note how the matching is increased in the urban path after the optimization of the model. In Table 9 are shown fitness function values by considering only urbanized area. The evaluation function increase in all considered cases, in particular it rises from 0.82 to 0.91 for Sopra Urno debris flow with a larger number of buildings and streets.

5 Conclusions

This paper presents SCIDDICA-SS2 improvements for simulating the part of debris flows that invade the urban areas. The less precision, related to momentum, of this version in comparison with SCIDDICA-SS3 and LLUNPIY (Lupiano et al. 2015c) does not worsen simulations in urban areas, because there is a larger turbulence.

Validation has been carried out by simulating Sopra Urno debris flow occurred on October 1st, 2009 in the Giampilieri Superiore territory.

An accurate study was performed in order to obtain the most accurate reproduction of the observed event. A new sub-state is introduced in AMD, which encodes building data, so as to take into account of the cells that contain buildings and soil simultaneously. This means that elements at different heights coexist in the same cell. Such model extension adapts very well to this problem. In fact, simulation results of Giampilieri Superiore debris flows are first-rate and may be evaluated still better, because fitness function was applied to full area for partially flooded cells.

SCIDDICA is a semi-empirical model, whose parameters are fixed almost definitively in validation phase with the “equivalent fluid” hypothesis (Lupiano et al. 2015a). Its simulations may be compared with other simulations of the same event, which are performed by the continuous models FLO-2D (O’Brien and Julien 1988) and TRENT-2D (Ardizzone et al. 2012).

FLO-2D is a commercial code, adopted worldwide for debris flow phenomena modelling and delineating flood hazards. It is a pseudo 2-D model in space which adopts

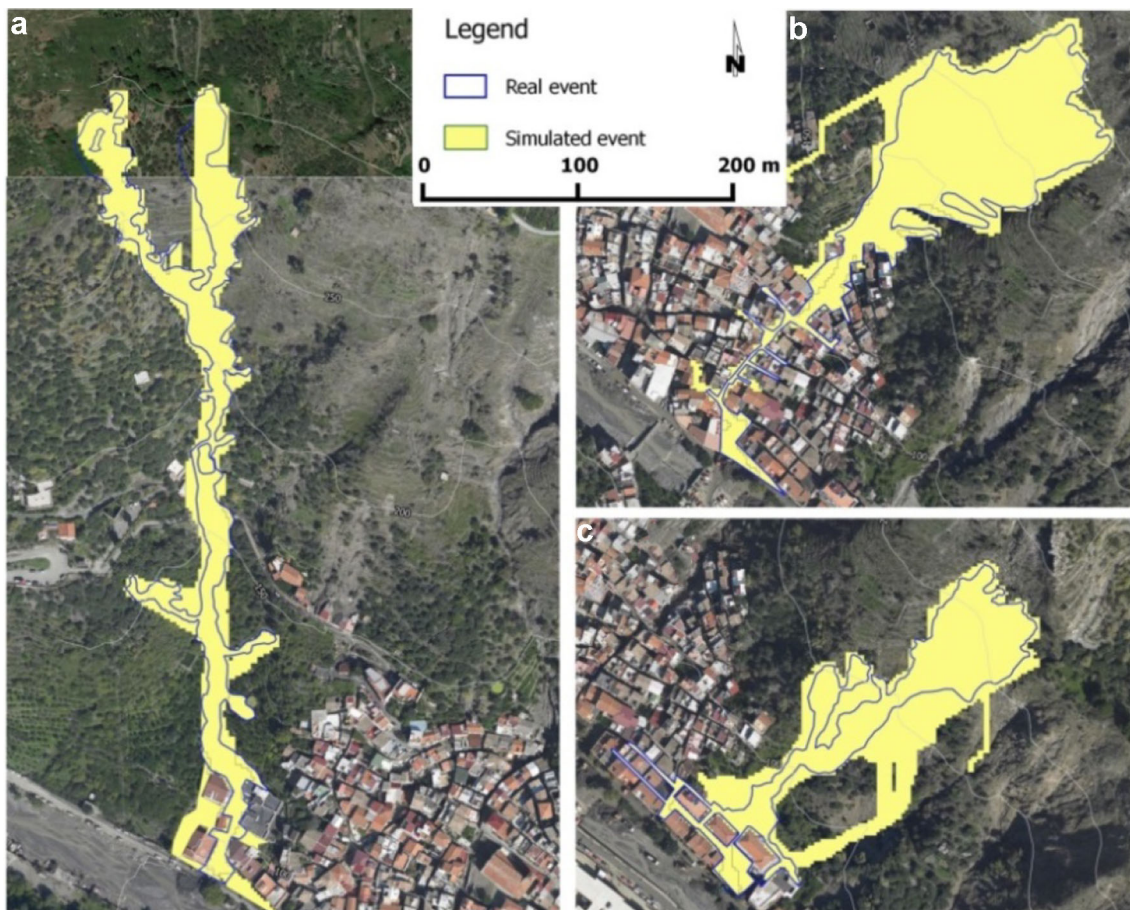


Fig. 6 Simulated events on DEM without improvements. **a** Loco creek debris flow; **b** Puntale Creek debris flow; **c** Lena Street debris flow

depth-integrated flow equations. Hyperconcentrated sediment flows are simulated considering the flow as a monophasic non-linear Bingham fluid. The basic equations implemented in the model consist mainly of the continuity equation; in FLO-2D the bed is fixed and all the debris mass is initially available (the erosion is not considered) (O'Brien and Julien 1988). Larger Giampileri Superiore's areas are covered in FLO-2D simulations in comparison with the real event and SCIDDICA results.

TRENT-2D is a code developed for the simulation of hyperconcentrated sediment transport and debris flows. It is based on a two-phase approach, in which the interstitial fluid is water and the granular phase is modelled according to the dispersive pressure theory of Bagnold, applied to the debris flows. The reference model has a more specific physical base, it is biphasic and able to reproduce the erosion and deposition processes. Small areas, which were

invaded in the real event and in SCIDDICA simulation, result untouched in TRENT-2D simulation and vice versa.

SCIDDICA simulations start from detachment area and continue considering erosion before town invasion; results about this first phase lack for both the results of FLO-2D and TRENT-2D.

A comment: the physical based simulations cannot very well take into account the soil anthropic influence. Giampileri Superiore's area was cultivated until recently, according to ancient agricultural techniques of terracing and control of surface runoff; the abandonment of this cultural heritage has not changed significantly the composition of the soil and didn't involve appreciable variations in the morphology before the 2009 events, but it has greatly enhanced the natural hazard.

The new features of SCIDDICA-SS2 could be very important for hazard and risk analyses in threatened towns by

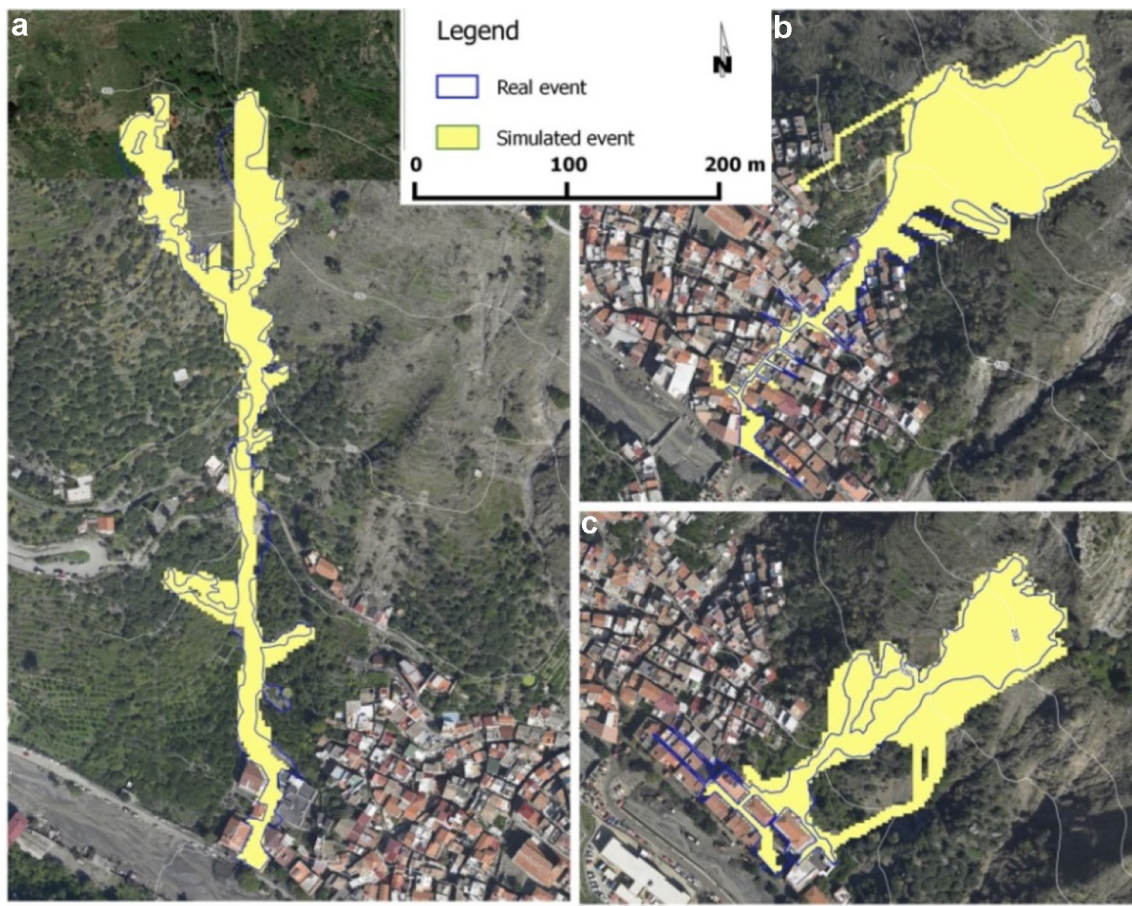


Fig. 7 Simulated events on DEM with improved model. **a** Loco creek debris flow; **b** Puntale Creek debris flow; **c** Lena Street debris flow

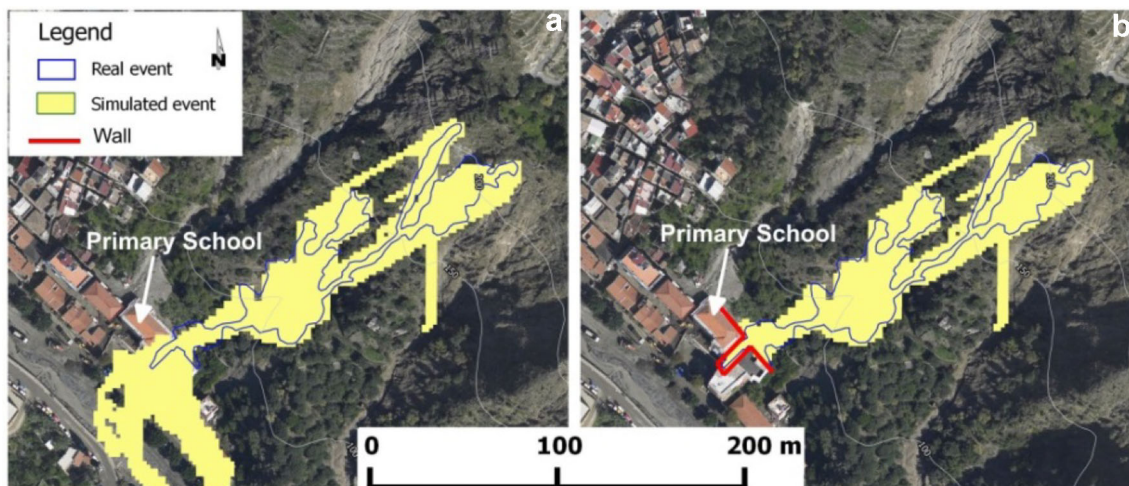


Fig. 8 Primary school debris flow. **a** Simulation without wall; **b** simulation with wall

flow-like landslides after a calibration of its parameters on real events, occurred in their territory. The efficiency of possible hazard mitigation works could also be tested by simulations.

The next important goal is modelling situations, where part of debris flows runs into tunnels (or channels modified in tunnel), that cross the urban area.

Table 8 Evaluation function f in debris flow used for validation of improvements

Case	$f = \sqrt{\frac{R \cap S}{R \cup S}}$ on DEM without improvement	$f = \sqrt{\frac{R \cap S}{R \cup S}}$ on DEM with improvement
1-Loce creek debris flow	0.79	0.79
3-Puntale creek debris low	0.85	0.86
4-Lena street debris flow	0.70	0.75

Table 9 Evaluation function f in urbanized area

Case	$f = \sqrt{\frac{R \cap S}{R \cup S}}$ on DEM without improvement	$f = \sqrt{\frac{R \cap S}{R \cup S}}$ On DEM with improvement
1-Loce Creek debris flow	0.69	0.88
2-Sopra Urno Creek debris flow	0.71	0.91
3-Puntale Creek debris low	0.70	0.73
4-Lena Street debris flow	0.55	0.74

References

- Arai K, Basuki A (2010) Simulation of hot mudflow disaster with cell automaton and verification with satellite imagery data. *Int Arch Photogramm Remote Sens Spat Inf Sci* 38(part 8):237–242
- Ardizzone F, Basile G, Cardinali M et al (2012) Landslide inventory map for the Briga and the Giampilieri catchments, NE Sicily, Italy. *J Maps* 8(2):176–180
- Avolio MV, Lupiano V, Mazzanti P, Di Gregorio S (2008) Modelling combined subaerial-subaqueous flow-like landslides by cellular automata. In: Umeo H, Morishita S, Nishinari K, Komatsuzaki T, Bandini S (eds) *Cellular automata, LNCS*, vol 5191. Springer, Berlin, pp 329–336
- Avolio MV, Di Gregorio S, Spataro W, Trunfio G (2012) A Theorem about the algorithm of minimization of differences for multicomponent cellular automata. In: Sirakoulis G, Bandini S (eds) *Cellular automata, LNCS*, vol 7495. Springer, Berlin, pp 289–298
- Avolio MV, Di Gregorio S, Lupiano V, Mazzanti P (2013) SCIDDICA-SS3: a new version of Cellular Automata model for simulating fast moving landslides. *J Supercomput* 65(2):682–696
- Avolio MV, Errera A, Lupiano V, Mazzanti P, Di Gregorio S (2017) A cellular automata model for snow avalanches. *J Cell Automata* 12(5):309–332
- Barca D, Di Gregorio S, Nicoletta F, Sorriso-Valvo M (1987) Flow-type landslide modelling by Cellular Automata. In: *Proceedings of AMS interbational congress on modelling and simulation*, Cairo, Egypt, pp 3–7
- Barpi F, Borri-Brunetto M, Veneri LD (2007) Cellular-automata model for dense-snow avalanches. *J Cold Reg Eng* 21(4):121–140
- Calidonna CR, Di Gregorio S, Gullace F, Gulli D, Lupiano V, Simos T, Tsitouras C (2016) RUSICA initial implementations: simulation results of sandy shore evolution in Porto Cesareo, Italy. In: *AIP conference proceedings*, vol 1738. AIP Publishing, p 480103. doi:10.1063/1.4952339
- Canuti P, Casagli N, Catani F, Falorni G (2002) Modeling of the Guagua Pichincha Volcano (Ecuador) lahars. *Phys Chem Earth A B C* 27(36):1587–1599
- Crisci GM, Di Gregorio S, Rongo R, Spataro W (2005) PYR: a cellular automata model for pyroclastic flows and application to the 1991 Mt. Pinatubo eruption. *Future Gener Comput Syst* 21(7):1019–1032
- Crisci GM, Iovine G, Di Gregorio S, Lupiano V (2008) Lava-flow hazard on the SE flank of Mt. Etna (southern Italy). *J Volcanol Geoth Res* 177(4):778–796
- Crisci GM, Avolio MV, Behncke B, D'Ambrosio D, Di Gregorio S, Lupiano V, Neri M, Rongo R, Spataro W (2010) Predicting the impact of lava flows at Mount Etna, Italy. *J Geophys Res Solid Earth* 115(B4):1–14
- D'Ambrosio D, Di Gregorio S, Gabriele S, Gaudio R (2001) A cellular automata model for soil erosion by water. *Phys Chem Earth B* 26(1):33–39
- D'Ambrosio D, Iovine G, Lupiano V, Rongo R, Spataro W, Bongolan VP (2013a) Non-uniform grid-based susceptibility evaluations: an application to flow-type phenomena at Mount Etna. *Rendiconti Online Della Società Geologica Italiana* 24:79–81
- D'Ambrosio D, Spataro W, Rongo R, Iovine G (2013b) Genetic algorithms, optimization, and evolutionary modeling. In: JF Shroder, ACW Baas (eds) *Treatise on geomorphology*. Academic Press, Cambridge, pp 74–97. doi:10.1016/B978-0-12-374739-6.00033-6
- Di Gregorio S, Serra R (1999) An empirical method for modelling and simulating some complex macroscopic phenomena by cellular automata. *Future Gener Comput Syst* 16(2):259–271
- Hung O (2009) Numerical modelling of the motion of rapid, flow-like landslides for hazard assessment. *KSCE J Civ Eng* 13(4):281–287
- Iovine G, Di Gregorio S, Sheridan MF, Miyamoto H (2007) Modelling, computer-assisted simulations, and mapping of dangerous phenomena for hazard assessment. *Environ Model Softw* 22(10):1389–1391
- Lupiano V, Avolio M, Di Gregorio S, Peres D, Stancanelli L (2014) Simulation of 2009 debris flows in the Peloritani mountains area by SCIDDICA-SS3. In: *Proceeding of 7th WSEAS international conference on engineering mechanics, structures, engineering geology*, Salerno (Italy), pp 53–61, ISBN: 978-960-474-376-6
- Lupiano V, Avolio MV, Anzidei M, Crisci GM, Di Gregorio S (2015a) Susceptibility assessment of subaerial (and/or) subaqueous debris flows in archaeological sites, using a cellular model. In: *Engineering geology for society and territory*. vol 8, pp 405–408. Springer. doi: 10.1007/978-3-319-09408-3_70
- Lupiano V, Machado G, Crisci GM, Di Gregorio S (2015b) A modelling approach with macroscopic Cellular Automata for hazard zonation of debris flows and lahars by computer simulations. *Int J Geol* 9:35–46. ISSN: 1998-4499
- Lupiano V, Peres D, Avolio M, Cancelliere A, Foti E, Spataro W, Stancanelli L, Di Gregorio S (2015c) Use of the SCIDDICA-SS3 model for predictive mapping of debris flow hazard: an example of application in the Peloritani mountains area. In: *Proceedings*

- of the international conference on parallel and distributed processing techniques and applications (PDPTA), pp 625–631
- Lupiano V, Machado G, Crisci GM, Di Gregorio S (2016) Simulations of debris/mud flows invading urban areas: a cellular automata approach with SCIDDICA. In: El Yacoubi S, Was J, Bandini S (eds) Cellular automata, LNCS, vol 9863. Springer, Berlin, pp 291–302
- Machado G, Lupiano V, Avolio M, Gullace F, Di Gregorio S (2015a) A Cellular model for secondary lahars and simulation of cases in the Vascún Valley, Ecuador. *J Comput Sci* 11:289–299
- Machado G, Lupiano V, Crisci GM, Di Gregorio S (2015b) LLUNPIY preliminary extension for simulating primary lahars application to the 1877 cataclysmic event of Cotopaxi Volcano. *SIMULTECH* 2015:367–376. doi:[10.5220/0005542903670376](https://doi.org/10.5220/0005542903670376)
- Mazzanti P, Bozzano F, Avolio MV, Lupiano V, Di Gregorio S (2010) 3D numerical modelling of submerged and coastal landslide propagation. In: Mosher DC, Shipp RC, Moscardelli L, Chaytor JD, Baxter CDP, Lee HJ, Urgeles R (eds) Submarine mass movements and their consequences IV; Advances in natural and technological hazards research, vol 28. Springer, Dordrecht, pp 127–139. doi:[10.1007/978-90-481-3071-9](https://doi.org/10.1007/978-90-481-3071-9)
- O'Brien JS, Julien PJ (1988) Laboratory analysis of mudflow properties. *Journal of Hydraulic Engineering, ASCE* 114(8):877–887
- Salles T, Lopez S, Cacas M, Mulder T (2007) Cellular Automata model of density currents. *Geomorphology* 88(1):1–20
- Stancanelli L, Foti E (2015) A comparative assessment of two different debris flow propagation approaches-blind simulations on a real debris flow event. *Nat Hazards Earth Syst Sci* 15(4):735–746
- Stancanelli L, Bovolin V, Foti E (2013) Application of a dilatant-viscous plastic debris flow model in a real complex situation. River, Coastal and Estuarine Morphodynamics: RCEM2011. Tsinghua University Press, Beijing, pp 74–97
- Valette G, Prevost S, Lucas L, Léonard J (2006) Soda project: a simulation of soil surface degradation by rainfall. *Comput Graph* 30(4):494–506
- Vanwallegem T, Jiménez-Hornero F, Giráldez J, Laguna A (2010) Simulation of long term soil redistribution by tillage using a cellular automata model. *Earth Surf Proc Land* 35(7):761–770. doi:[10.1002/esp.1923](https://doi.org/10.1002/esp.1923)